Response of an electrostatic probe for a right cylindrical spacer

Rerup, T; Crichton, George C; McAllister, Iain Wilson

Published in:
IEEE Annual Report., Conference on Electrical Insulation and Dielectric Phenomena

Link to article, DOI:
10.1109/CEIDP.1994.591737

Publication date:
1994

Document Version
Publisher's PDF, also known as Version of record

RESPONSE OF AN ELECTROSTATIC PROBE FOR A RIGHT CYLINDRICAL SPACER

T.O. Rerup, G.C. Crichton and I.W. McAllister

Electric Power Engineering Department
Building 325
The Technical University of Denmark
DK-2800 Lyngby, Denmark

INTRODUCTION

During the last decade many experimental studies of surface charge phenomena have been undertaken employing right cylindrical spacers. Measurement of the surface charge was performed using small electrostatic field probes to scan across the dielectric surface. Owing to mechanical requirements, each probe consists essentially of a long cylindrical shaft at earth potential, with a circular conducting disc insulated from but mounted coaxially at the end of the shaft. The potential of this disc/sensor-plate is floating. Charges are electrostatically induced on the sensor plate by the ambient surface charge, and hence as the probe is moved parallel to the surface the potential of the sensor plate changes. The probe sensor-plate potential is thus the parameter of interest as this parameter can be related in a quantitative manner to the surface charge density.

To facilitate a proper evaluation and interpretation of such probe measurements, Pedersen introduced a probe response function, the λ-function [1]. In the present study, the influence of the spacer geometry upon the λ-function is examined. This knowledge allows the response of the probe with reference to detection sensitivity and spatial selectivity to be considered. Such probe characteristics enable general conclusions to be reached about the interpretation of experimental studies.

THE λ-FUNCTION

Pedersen's λ-function relates the charge induced on the probe to the surface charge density at the dielectric in-

terface [1]. If it is assumed that the volume charge density within the solid dielectric is *zero*, then this relationship can be expressed as

$$q = -\iint_{A_o} \lambda \sigma dA \tag{1}$$

where q is the Poissonian induced-charge on the sensor plate [2]; σ is the surface charge density on the surface element dA of A_o, the surface of the solid dielectric.

The dimensionless parameter λ is a solution of the general Laplace equation for the complete measuring geometry;

$$\vec{\nabla} \cdot (\varepsilon \vec{\nabla} \lambda) = 0 \tag{2}$$

The boundary conditions are $\lambda = 1$ at the probe sensor-plate and $\lambda = 0$ at all other electrodes. In addition, at the dielectric interface the normal derivatives of λ must obey the condition

$$\varepsilon_+ (\frac{\partial \lambda}{\partial n})_+ = \varepsilon_- (\frac{\partial \lambda}{\partial n})_- \tag{3}$$

where the + and - signs refer to the opposite sides of the interface [1]. As (2) is just Laplace's equation, any standard method of solving this equation can be used to evaluate the variation of λ at the surface. On this occasion, the solutions were obtained using an Ansoft 2-D finite-element software package. These solutions are then utilised to study the dependence of the λ-function upon the system geometry.

SYSTEM GEOMETRY

The geometry of the probe has been described in [3,4]. The essential parameters are the radius of the sensor plate r and the outer radius of the probe guard ring R. The probe is positioned perpendicular to the planar end-faces of a right cylindrical spacer, at a height h above an end-face, see Fig.1. As previously, we take $R = 6r$ and $h = 0.5r$.

The dielectric spacer, of relative permittivity ε_r, has a

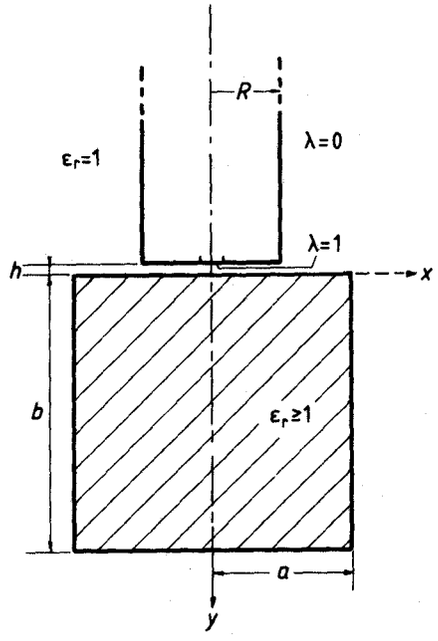

Fig.1. The system geometry

height b in a direction parallel to the probe axis, while in the normal direction the diameter of the spacer is $2a$, see Fig.1, in which x,y represent cylindrical coordinates. In the present study, we select $a = 2R$ and $b = 4R$.

RESULTS AND DISCUSSION

General Situation

For the present spacer geometry, three gas/solid dielectric interfaces can be identified. To distinguish between these, we will identify the near interface with the subscript 'n', the side interface with the subscript 's' and the far interface with the subscript 'f'. The variation of λ along these interfaces is illustrated in Fig.2 for $b/a = 2$ and $\varepsilon_r = 4$. This diagram indicates clearly that the major difference between λ_n and λ_f occurs in the region beneath the probe, i.e. in the lateral range $x \leq R$. In this range, the magnitude of λ_n decreases by a factor

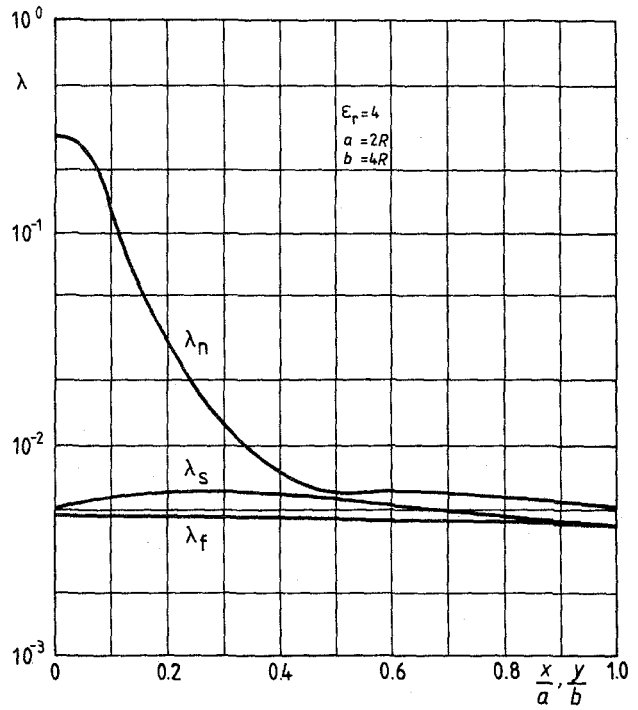

Fig.2. Variation of $\lambda_n(x)$, $\lambda_f(x)$ and $\lambda_s(y)$

of ~50, whereas, with a reduction of <3%, λ_f is essentially constant. Although the magnitudes of λ_f and λ_s are comparable, the distribution of these functions is quite different; viz. λ_f falls monotonically from a maximum value on the axis while λ_s exhibits a maximum value at $y = 0.25b$.

The results of similar λ-calculations for other values of ε_r are listed in Table 1. For increasing ε_r-values, $\lambda_n(0)$ displays a marked reduction, while the opposite trend is observed for $\lambda_n(R)$, $\lambda_n(2R)$ and λ_f. The values of λ_s are not tabulated as these lie in the range $\lambda_n(2R) \leqq \lambda_s \leqq \lambda_f(2R)$, with a maximum at $y \sim 0.25b$. As $\varepsilon_r = 1$ represents a situation with no polarisable material, λ-values for $\varepsilon_r > 1$ must reflect the influence of dielectric polaris-

Table 1. $\lambda_n(x)$ and $\lambda_f(x)$ data for different ε_r

ε_r	$\lambda_n(0)$	$\lambda_n(R)$	$\lambda_n(2R)$
1	0.570	1.93(-3)	1.68(-3)
2	0.427	3.63(-3)	3.09(-3)
4	0.290	6.02(-3)	5.19(-3)
6	0.221	7.52(-3)	6.63(-3)
ε_r	$\lambda_f(0)$	$\lambda_f(R)$	$\lambda_f(2R)$
1	1.48(-3)	1.40(-3)	1.20(-3)
2	2.76(-3)	2.64(-3)	2.32(-3)
4	4.71(-3)	4.58(-3)	4.14(-3)
6	6.09(-3)	5.96(-3)	5.51(-3)

Note (-3) $\equiv 10^{-3}$

ation. Evidence for this behaviour is clearly found in Table 1.

Although the $\lambda_n(0)$-values may appear to be the only significant ones, this is not the complete picture with respect to the magnitude of the induced-charge. This aspect will now be quantified. For a disc of constant surface charge density σ_o located at a planar dielectric interface, the induced charge q on the sensor plate is given by

$$q(x) = 2\pi\sigma_o \int_0^x \lambda(x',y)x'\,dx' \tag{4}$$

where x' is a dummy variable, and a constant y represents a planar (end-face) interface. In discussing the variation of $q(x)$, it proves convenient to introduce a normalized detection sensitivity $S_e(x)$ defined by

$$S_e(x) = \frac{2}{R^2} \int_0^x \lambda(x',y)x'\,dx' \tag{5}$$

Similarly, by considering a cylindrical shell of constant surface charge density σ_o located at the cylindrical interface, we obtain the associated induced-charge and the corresponding detection sensitivity, viz.

$$q(y) = 2\pi a\sigma_o \int_0^y \lambda(a,y')dy' \tag{6}$$

$$S_e(y) = \frac{2a}{r^2} \int_0^y \lambda(a,y')dy' \tag{7}$$

where y' is a dummy variable.

The variations of S_e for the different interfaces are shown in Fig.3. For large areas of charge, this figure indicates that the induced-charge contributions from the near and side interfaces are more significant than that from the far interface. The latter is however not insignificant. With respect to the influence of ε_r, the relevant S_e-values are given in Table 2. Although $S_{en}(x)$ decreases with increasing ε_r, the existence of the product $\lambda(x,y)x$ in the integral of (5) has diminished the influence of the peakiness of the $\lambda_n(x)$-distribution. All the other S_e-values increase with ε_r. The above S_{en} behaviour indicates that, for the same charged area, the percentage of the recorded signal due to charge outwith the area subtended directly by the probe ($x \leq R$, $y = 0$) will increase with ε_r. Interpretation of the induced-charge signal is further complicated by contributions from the side and far interfaces.

Mathematically it is possible to consider the induced-charge component from each interface separately, and thus obtain an indication of the probe response. In practice, only the net induced-charge is measured; i.e. the sum of the near, side and far interface components. In such a situation a valid interpretation of the probe signal can only be obtained through the use of a scanning procedure.

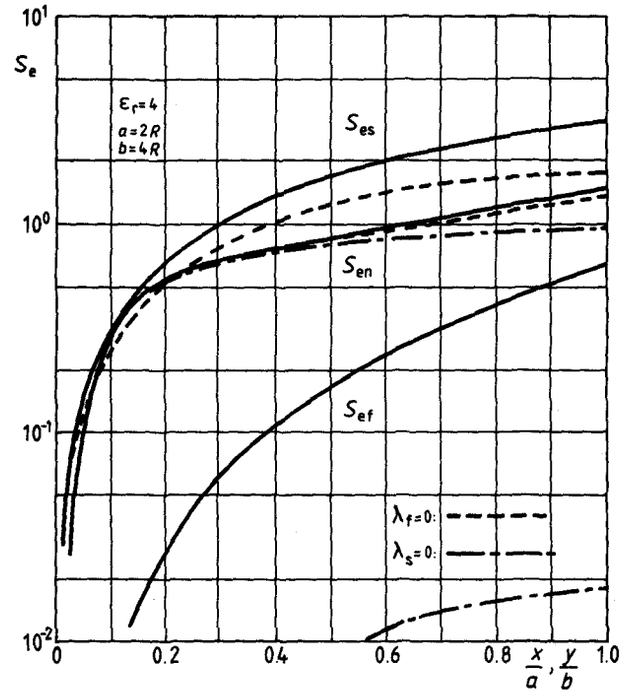

Fig.3. Variation of $S_{en}(x)$, $S_{ef}(x)$ and $S_{es}(y)$

Table 2. $S_{en}(x)$, $S_{ef}(x)$ and $S_{es}(y)$ data for different ε_r

ε_r	$S_{en}(R)$	$S_{en}(2R)$	$S_{ef}(R)$	$S_{ef}(2R)$
1	1.016	1.229	0.052	0.191
2	0.950	1.333	0.097	0.365
4	0.855	1.476	0.167	0.639
6	0.791	1.567	0.217	0.838

ε_r	$S_{es}(R)$	$S_{es}(2R)$	$S_{es}(3R)$	$S_{es}(4R)$
1	0.309	0.642	0.906	1.106
2	0.533	1.089	1.551	1.924
4	0.840	1.694	2.442	3.087
6	1.040	2.086	3.029	3.872

Table 3. $\lambda_n(x)$, $\lambda_f(x)$ and $\lambda_s(y)$ data for $\varepsilon_r = 4$

condition	$\lambda_n(0)$	$\lambda_n(R)$	$\lambda_n(2R)$
general	0.290	6.02(-3)	5.19(-3)
$\lambda_f = 0$	0.289	5.38(-3)	4.11(-3)
$\lambda_s = 0$	0.288	3.62(-3)	0
	$\lambda_f(0)$	$\lambda_f(R)$	$\lambda_f(2R)$
general	4.71(-3)	4.48(-3)	4.14(-3)
$\lambda_s = 0$	2.79(-4)	1.89(-4)	0
	$\lambda_s(R)$	$\lambda_s(2R)$	$\lambda_s(3R)$
general	6.13(-3)	5.60(-3)	4.81(-3)
$\lambda_f = 0$	4.57(-3)	3.37(-3)	1.77(-3)

Note $\lambda_s(0) = \lambda_n(2R)$, $\lambda_s(4R) = \lambda_f(2R)$

Specific Situations

Depending on experimental conditions, it is possible that either $\lambda_f = 0$ or $\lambda_s = 0$. We will now briefly examine the properties of such conditions.

For $\lambda_f = 0$, the spacer is placed on an earthed conducting disc of radius a. Specific values of λ_n and λ_s are listed in Table 3, from which it is evident that the major change in λ_n occurs for $x > R$. Although $\lambda_s \to 0$ as $y \to 4R$, Table 3 indicates that, as $\lambda_s(y) > \lambda_s(0)$ for $y < 2R$, λ_s still exhibits a maximum value. The effects of the above changes in λ_n and λ_s upon S_e are illustrated in Fig.3, from which it is clear that the maximum change in S_e ($\sim 40\%$) occurs with S_{es} in the vicinity of the $\lambda_f = 0$ boundary. For S_{en} the maximum reduction is <10%.

For $\lambda_s = 0$, the spacer is placed within an earthed conducting cylindrical shell of radius a and length b. Relevant λ-values are given in Table 3, while the appropriate S_e are included in Fig.3. As $\lambda_n \rightarrow 0$ as $x \rightarrow 2R$, an even greater change occurs in λ_n for $x > R$ and this is clearly reflected in S_{en}. On this occasion, $\lambda_f < 0.0003$ such that now $S_{ef} < 0.02 S_{en}$, see Fig.3.

CONCLUSION

Although restricted to an axial configuration, the present study of the probe λ-function associated with a right cylindrical spacer has elucidated the essential characteristics of such a surface charge measuring system. The study indicates that contributions to the induced-charge from areas outwith that immediately subtended by the probe can account for a major portion of the probe signal.

The major influence of dielectric polarisation upon the induced-charge is highlighted. Although dependent upon the relative permittivity of the spacer dielectric, the effect is also related to the probe location relative to the surface area of the near interface.

The existence of local $\lambda = 0$ electrode boundaries is shown to reduce the induced-charge contributions from less immediate areas and other interfaces of the spacer, without significantly affecting the contribution from directly under the probe. Hence, if possible, such boundaries should be used during probe measurements, as these will improve the spatial selectivity of the probe.

Finally, it must be concluded that, to undertake a reliable evaluation of experimental measurements, it is necessary to possess a complete knowledge of the λ-function for the probe/spacer-geometry in question. This knowledge is combined with measurements obtained from scanning across the interfaces of the spacer to yield the unknown surface charge distribution.

REFERENCES

[1] A. Pedersen, "On the Electrostatics of Probe Measurements of Surface Charge Densities", in L.G. Christophorou and D.W. Bouldin, *Gaseous Dielectrics V*, New York: Pergamon Press 1987, pp.235-240.

[2] A. Pedersen, G.C. Crichton and I.W. McAllister, "Partial Discharge Detection: Theoretical and Practical Aspects", International Conference on Partial Discharge, Canterbury 1993. IEE Conference Proceedings No.378, pp.21-24, 1993.

[3] T.O. Rerup, G.C. Crichton and I.W. McAllister, "The Response of Electrostatic Probes via the λ-Function", Conference Record of the 1994 IEEE International Symposium on Electrical Insulation, Pittsburgh 1994. IEEE Publication 94CH3445-4, pp.82-88, 1994.

[4] T.O. Rerup, G.C. Crichton and I.W. McAllister, "The λ-function and the Response of Electrostatic Probes", NORD-IS 94, Nordic Insulation Symposium, Vaasa, Finland 1994, Paper No.7.7, 9pp.